# Electron Cloud Modeling Results for Time-Resolved Shielded Pickup Measurements at CesrTA


J.A. Crittenden, Y. Li, X, Liu, M.A. Palmer, J.P. Sikora
CLASSE*, Cornell University, Ithaca, NY 14850, USA

S. Calatroni, G. Rumolo
CERN, Geneva, Switzerland

N. Omcikus
University of California at Los Angeles, Los Angeles, CA 90095-1597



*Abstract*

The Cornell Electron Storage Ring Test Accelerator (CesrTA) program [1] includes investigations into electron cloud buildup, applying various mitigation techniques in custom vacuum chambers. Among these are two 1.1-m-long sections located symmetrically in the east and west arc regions. These chambers are equipped with pickup detectors shielded against the direct beam-induced signal. They detect cloud electrons migrating through an 18-mm-diameter pattern of holes in the top of the chamber. A digitizing oscilloscope is used to record the signals, providing time-resolved information on cloud development. Carbon-coated, TiN-coated and uncoated aluminum chambers have been tested. Electron and positron beams of 2.1, 4.0 and 5.3 GeV with a variety of bunch populations and spacings in steps of 4 and 14 ns have been used. Here we report on results from the ECLOUD modeling code which highlight the sensitivity of these measurements to model parameters such as the photoelectron azimuthal and energy distributions at production, and the secondary yield parameters including the true secondary, rediffused, and elastic yield values. In particular, witness bunch studies exhibit high sensitivity to the elastic yield by providing information on cloud decay times.


## INTRODUCTION

The CesrTA program includes the installation of custom vacuum chambers with retarding-field-analyzer (RFA) ports and shielded pick-up detectors of the type shown in Fig. 1. The RFA port is shown on the left end, and two circular shielded pickup modules are shown on the right end of the chamber, each with two ports. In one case the two ports are placed longitudinally, with only one of the two being read out, and in the other case the two ports are arranged transversely, providing laterally segmented sensitivity to the cloud electrons. Thus the centers of buttons are 0, and $\pm 14$ mm from the horizontal center of the chamber. The ports consist of 169 30-mil-diameter holes arranged in concentric circles up to a maximum diameter of 18 mm. The top of the vacuum chamber has been machined such that the holes point vertically. The transparency factor for vertical trajectories is 27%. The approximate 3:1 depth-to-diameter factor is chosen to effectively shield the detectors from the signal induced directly by the beam.

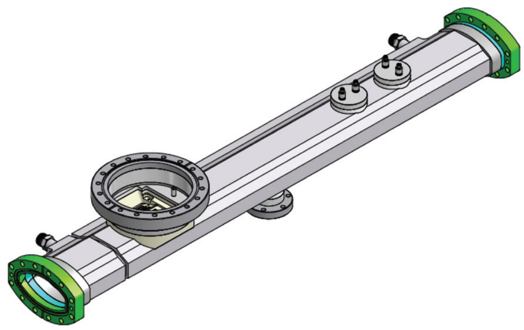

Figure 1: Custom vacuum chamber with RFA port and shielded pickup detectors.

Time-resolved measurements provide time structure information on cloud development, in contrast to the time-integrated RFA measurements [2]. However, they have relatively primitive energy selection, since they have no retarding grid and position segmentation is more coarse, the charge-collecting electrodes being of diameter 18 mm. Data has been recorded with biases of 0 and $\pm 50$V relative to the vacuum chamber. The studies described here address exclusively the data a with bias $+50$ V in order to avoid contributions to the signal from secondary electrons escaping the pickup. Such secondaries generally carry kinetic energy insufficient to escape a 50 V bias. This choice of bias obviously provides sensitivity to cloud electrons which enter the port holes with low kinetic energy. The front-end readout electronics comprise operational amplifiers with 50 $\Omega$ input impedance and a gain factor of 100. Digitized oscilloscope traces are recorded with 0.1 ns step size.

## USE OF A WEAK SOLENOIDAL MAGNETIC FIELD

One type of measurement which has been obtained with the shielded-pickup detectors is illustrated schematically


* Work supported by the U.S. National Science Foundation, the U.S. Department of Energy, and the Japan/USA Cooperation Program

in Fig. 2. The vacuum chambers have been outfitted with windings to approximate a solenoidal field in the region of the cloud with magnitude up to 40 G. Since signal contributions require nearly vertical arrival angles, the centers of the corresponding circular trajectories for any given magnetic field value lie in the horizontal plane of the ports. The three trajectories originating at the primary impact point of the synchrotron radiation and leading to the center of each electrode thus select different regions of photoelectron energy and production angle, as shown. Experiments to date

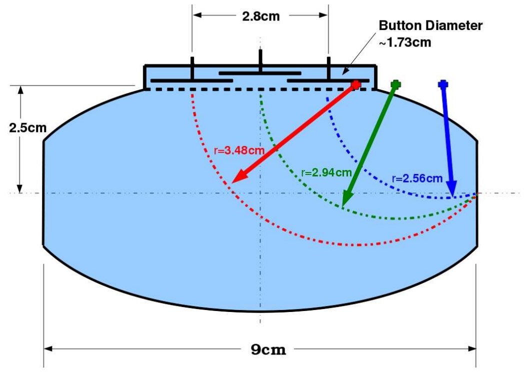


Figure 2: Vacuum chamber wall cross section with circular trajectories of photoelectrons contributing to the pickup signals.

have shown that the 40 G field magnitude range suffices to cover the full energy range of the photoelectrons produced by a 2.1 GeV beam ($E_{\mathrm{critical}} \approx 300$ eV) (i.e. no pickup signal is observed for field values of 0 and 40 G), in contrast to the case of a 5.3 GeV beam ($E_{\mathrm{critical}} \approx 5$ keV), where photoelectron energies suffice to produce an observable signal even at 40 G. Furthermore, reversal of the solenoidal field provides information on the production of photoelectrons at a point on the vacuum chamber opposite the primary source point and thus relevant to the reflective characteristics of the vacuum chamber wall. This paper does not discuss in detail the measurements obtained with solenoidal field, which remain under analysis, but instead concentrates on an alternative method to measure photoelectron energy.

## SENSITIVITY TO PHOTOELECTRON ENERGY DISTRIBUTION

The upper row of Fig. 3 shows examples of shielded pickup signals for two bunches of 5.3 GeV positrons (left) and electrons (right) separated by 14 ns. The population of the first bunch is 1.3E11e while that of the trailing bunch varies up to a similar value. The trailing bunch accelerates cloud particles into the detector, producing the second signal. The arrival time and structure of the earlier signal corresponds to photoelectrons produced at the time of bunch passage on the lower chamber wall. The kick from the positron bunch accelerates such photoelectrons toward the detector, whereas in the case of an electron beam the signal electrons must carry sufficient kinetic energy to overcome the repulsion of the beam bunch.

The lower row of Fig. 3 shows an initial attempt to model the case of two 1.3E11e bunches using the electron cloud simulation code ECLOUD [3]. The calculation of cloud kinematics including space charge forces and beam kicks determines arrival times, momentum vectors and charges of the macroparticles reaching the upper surface of the chamber at the positions of the pickups. This early attempt at simulating the observed signals included a rather crude model of the port hole acceptance, leading to poor approximation of the magnitude of the signal, but it was sufficient to diagnose the obviously discrepancy with the observed signals. The positron case shows moderate time structure differences, but the modeling of the electron beam kick exhibited a dramatic discrepancy. The arrival times of the observed signals indicate photoelectron production on the lower wall of the chamber, which is effected in the simulation via a reflectivity parameter distributing 20% of the photoelectrons uniformly in azimuth. The prompt signal from each electron bunch corresponds to photoelectrons produced on the upper wall repelled into the detector during the bunch passage. The photoelectrons produced on the lower wall in the ECLOUD simulation are similarly reabsorbed, and these are the ones needed to produce the observed signal! In other words, the measurement shows that photoelectrons of sufficient energy to overcome the repulsion of the beam bunch must be present. The photoelectron energy distribution in this original default model is common to many successful simulations of a wide variety of experimental observations [3, 4, 5], namely a Gaussian with average and rms values of 5 eV limited by truncation to positive values. Figure 4 compares such a distribution (blue) to a power-law modification adequately reproducing the observed signal shapes (red). Low-energy and high-energy regions are shown normalized on logarithmic scales to illustrate the dramatically higher energies needed.

This new high-energy distribution was determined by matching single-bunch models to the measured signals for various electron bunch currents as shown in Fig. 5. The measured signals for a single bunch of 5.3 GeV electrons are shown in the left column. A bunch current of 1 mA corresponds to a bunch population of 1.6E10e. The model successfully reproduces the increase of signal magnitude with bunch current. While some time structure discrepancies remain, the improvement relative to the results shown in Fig. 3 is remarkable. The overall normalization of the modeled signals is proportional to the assumed reflectivity value, which in this case was 20%. In addition, the model also exhibits a prompt signal arising from photoelectrons produced nearby the detector repelled into it during the passage of the bunch, increasing with bunch current similarly to the observed signals.

Extensive work continues on refining the energy distributions, studying the consequences on earlier successful modeling of various physical phenomena, and exploiting the information provided by data taken in solenoidal mag-

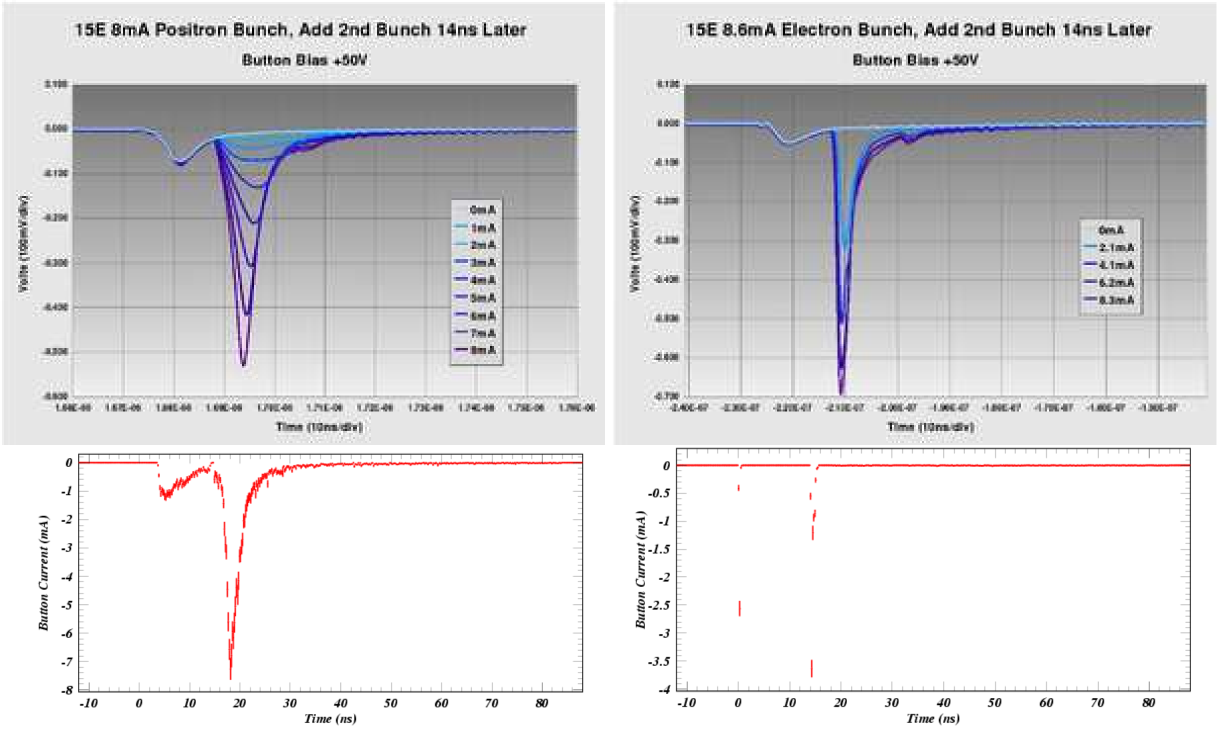


Figure 3: Upper row: shielded pickup signals produced by two 5.3 GeV positron (left) and electron (right) bunches separated by 14 ns. The leading bunch population is 1.3E11e . The population of the second bunch varies up to a similar value. Lower row: initial ECLOUD model results exhibiting discrepancies with the measured signals which are quite dramatic in the case of the electron beam.

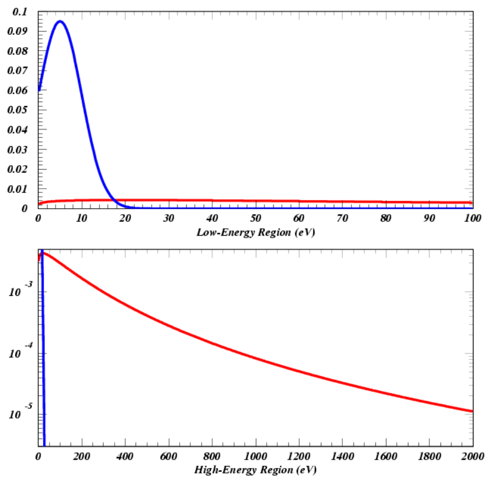


Figure 4: Low- and high-energy regions of the photoelectron energy distributions used to model the measured signals shown in Fig. 3. The original low-energy distribution shown in blue results in dramatic discrepancy with the signals observed in the case of an electron beam. The modified distribution shown in red provides good agreement with the observed signals.

netic fields.

This analysis presents an intriguing opportunity to relate the obtained photoelectron energy distribution to the incident synchrotron energy spectrum and thus derive an estimate of the energy dependence of the quantum efficiency. Since the source of the direct radiation at the primary point of incidence on the outside wall of the beampipe is well known, the critical energy is well defined. However, these signals do not arise from the direct radiation, but rather from a reflected portion of the spectrum. Detailed work on modeling reflected photon trajectories has been undertaken [6]. Preliminary results of this model [7] indicate that the energy dependence of the reflectivity results in an impact energy distribution for the reflected portion of the photon spectrum which is much lower than would be expected from the critical energy of the direct synchrotron radiation. It may be conjectured the high energies needed to explain the shielded pickup signals arise from an interaction of high-energy photons with the wall other than reflection.

## *Cloud Lifetime Studies Using Witness Bunches*

While the awareness of the sensitivity of the shielded pickup measurements to the parameters of photoelectron production was largely motivated by inadequacies of the model discovered in its application to recent measurements, the original intended use of these time-resolved cloud measurements was to provide a quantitative estimate of the elastic yield parameter in the secondary electron yield model. A similar investigation was performed

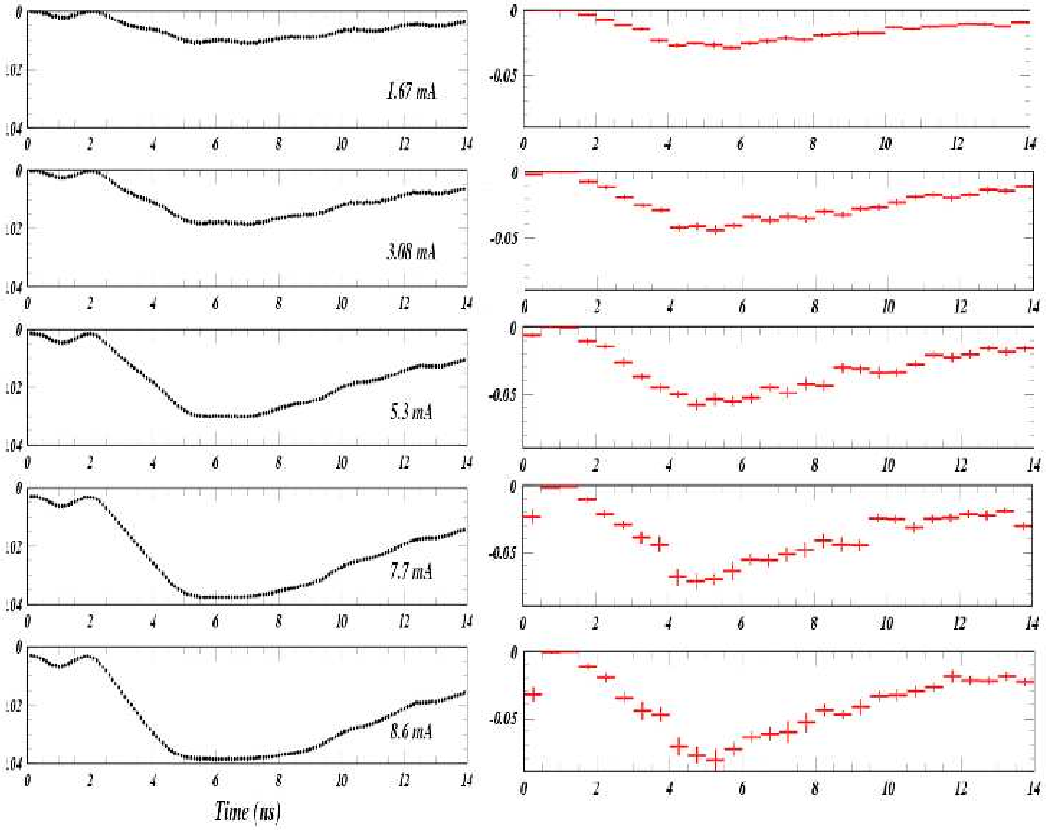


Figure 5: Comparison of measured single bunch signals for various electron bunch currents (left column) to the ECLOUD model (right column) after improving the modeled photoelectron energy distributions.

at RHIC [8]. The basic concept is that the mature cloud long after passage of any beam bunch is dominated by low-energy electrons which suffer predominantly elastic interactions with the vacuum chamber wall. The elastic yield parameter describes the ratio of outgoing to incoming macroparticle charge in probabilistic models [9], and carries a value typically 0.5-0.7, determining the decay time of the cloud density, typically around 100 ns. High-energy electrons of more than 100 eV, produced by synchrotron radiation, beam kicks, or the rediffused component of the secondary yield process, undergo primarily the so-called "true" secondary yield process, in which the produced secondary carries only a few electron volts of kinetic energy, resulting in the dominance of low-energy electrons late in the cloud development.

Figure 6 shows an ECLOUD secondary yield population curve typical of the shielded pickup signal simulations.The true secondary yield maximum at 400 eV ranges from a minimum of 0.9 to a maximum of 1.5 owing to the dependence on incident angle. At low energy the yield value is dominated by the elastic interactions with the chamber wall. This case exhibits an elastic yield parameter of 0.55.

The witness bunch experimental method consists of generating a cloud with a leading bunch, then accelerating cloud electrons into the shielded pickup detector with a trailing bunch at various delay times. The magnitude and time structure of the signal from the leading bunch is determined by the reflective properties of the vacuum chamber and by the energy-dependent quantum efficiency, as described in the preceding section. The signal induced by the witness bunch has a contribution similar to that of the leading bunch added to the contribution from the existing cloud kicked into the detector. The latter contribution is sensitive to the cloud density and the spatial and kinematic distributions of the cloud electrons. Figure 7 shows the results of six sets of simulations with various values for the elastic yield parameter $\delta_0$. In each of the six plots, eleven two-bunch (5.3 GeV, 4.8E10e positrons each) pickup signals are superposed, whereby the delay of the witness bunch varies from 12 to 100 ns. The modeled signals are shown with the statistical error bars corresponding to the number of macroparticles contributing to the signal. The magnitudes of the modeled signals at large witness bunch delay clearly show the dependence on the elastic yield parameter $\delta_0$ as it is varied from 0.05 to 0.75. The most consistent description of the measured signals is given by a value of $\delta_0 = 0.75$. This value can be compared to the value of $\delta_0 = 0.5$ used in the modeling of CesrTA coherent tune shift measurements as described in Refs. [4, 5], where the measurements had much less discriminating sensitivity to the elastic yield.

Figure 8 shows a similar study, but for a titanium-nitride-

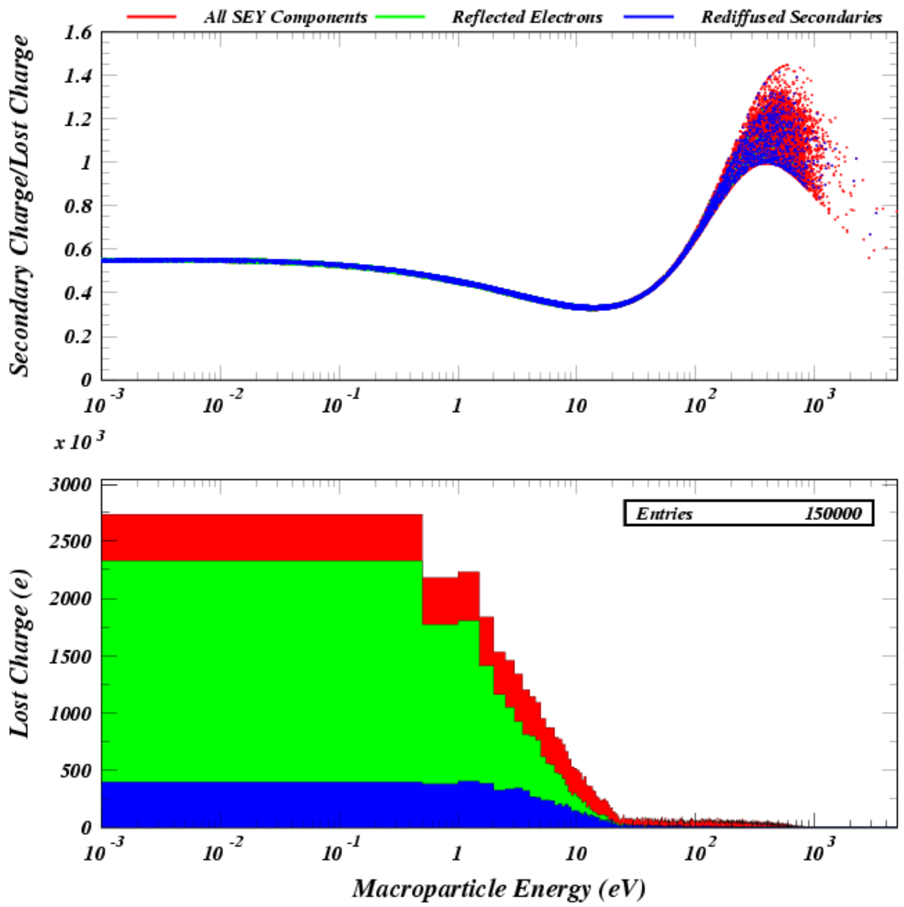


Figure 6: Secondary yield population curve typical of the ECLOUD model for the shielded pickup signals.The upper plot shows the yield value (ratio of secondary macroparticle charge to that of the incident charge) as a function of the incident kinetic energy. At low energy the yield value is dominated by the elastic interaction with the chamber wall. This case exhibits an elastic yield parameter of 0.55. The lower plot shows the incident energy distribution. The elastic and rediffused components are shown in green and blue, respectively. The sum of all three components, true, elastic and rediffused, is shown in red. Since the three colors are plotted on top of each other, the upper plot shows primarily blue at low energy, even though the elastic process dominates, as is seen in the lower plot.

coated aluminum chamber. For each of the six values assumed for the elastic yield, thirteen two-bunch (5.3 GeV, 8.0E10e positrons each) pickup signals are superposed, whereby the delay of the witness bunch is varied from 14 to 84 ns. The optimal value for the elastic yield is clearly less than the value determined for the uncoated aluminum chamber, with $\delta_0 = 0.05$ providing the best description of the measurements.

These comparisons show a number of intriguing discrepancies. The leading bunch signal shape exhibits the need for further tuning of the photoelectron energy distribution. The signal widths tend to be wider than observed. In addition, such a low value of 0.9 for the secondary yield of an uncoated aluminum surface cannot be easily understood, since the tune shifts measurements require an average value around the CESR ring of about 1.8. A wide variety of systematic studies have been undertaken since the ECLOUD'10 workshop, discovering sensitivity to many detailed characteristics of the cloud. For example, the signal widths for early witness signals depend strongly on the azimuthal production distribution of photoelectrons, as was observed by implementing in ECLOUD the distributions calculated by the photon-tracing reflectivity model for the CESR ring described in Ref. [6]. Nonetheless, the dramatic improvements in consistency obtained via such systematic studies have not changed the quantitative conclusions concerning the sensitivity to the value for the elastic yield. Generally one can say that the choice of peak true secondary yield value relative to the effective reflectivity value determines the ratio of the early witness bunch signal magnitudes to that from the leading bunch. However, for witness bunches late enough that the signal magnitude becomes comparable to that of the leading bunch, there is little sensitivity to the true secondary yield. Instead, those signal magnitudes are determined by the value assumed for the elastic yield.

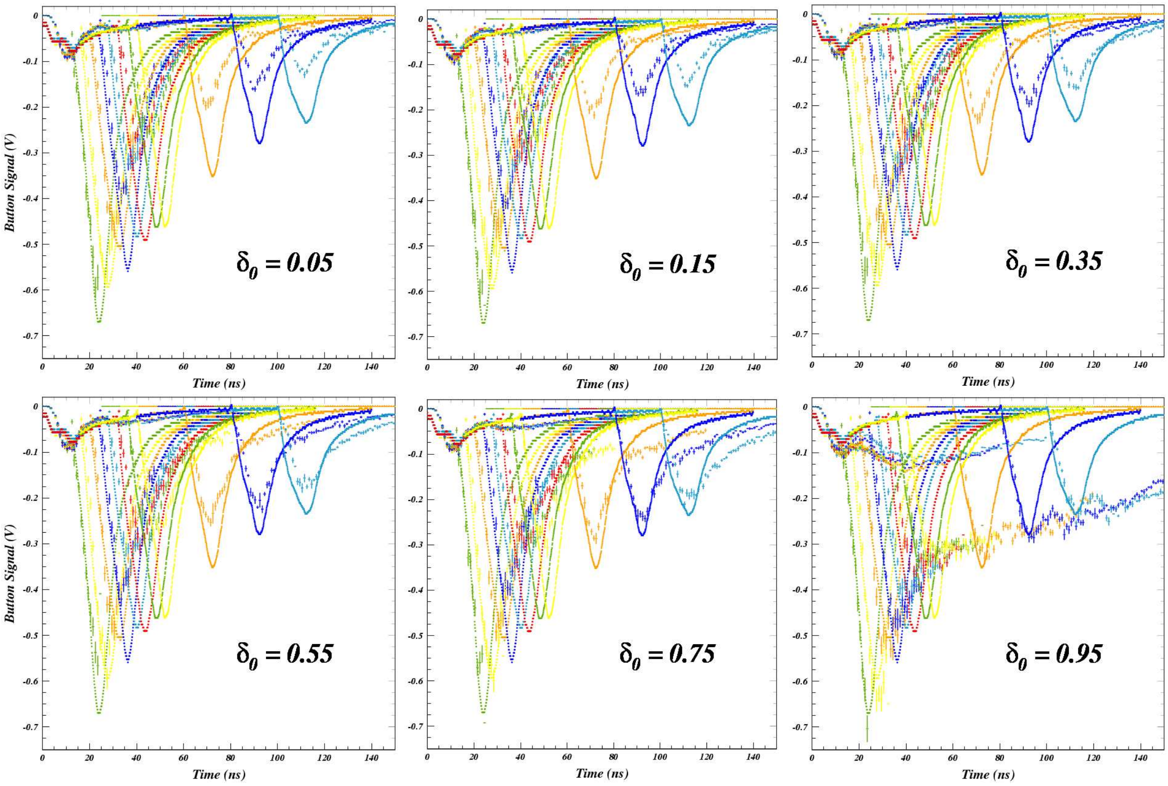


Figure 7: Witness bunch study with the uncoated aluminum chamber. Eleven two-bunch scope traces are superposed in each of the six plots, whereby the delay of the witness bunch ranges from 12 to 100 ns. The modeled signals are shown with the statistical error bars corresponding to the number of macroparticles contributing to the signal. The magnitudes of the modeled signals at large witness bunch delay clearly show the dependence on the elastic yield parameter $\delta_0$ as it is varied from 0.05 to 0.75. The most consistent description of the measured signals is given by a value of $\delta_0 = 0.75$.

## SUMMARY

The shielded pickup detectors installed in the CESR ring in 2010 have begun providing a wide variety of time-resolved measurements of electron-cloud-induced signals. Measurements with custom vacuum chambers incorporating cloud mitigation techniques such as carbon and titanium-nitride coatings have been obtained and compared to the case of an uncoated aluminum chamber. Weak solenoidal magnetic fields have been employed to study photoelectron production kinematics. A model for the shielded pickup acceptance has been developed in the context of the electron cloud simulation code ECLOUD. The shielded pickup data have proven remarkably sensitive to model parameters poorly constrained by any other experimental means, such as the azimuthal production distribution for photoelectrons and their energy distributions. The measurements with 5.3 GeV electron and positron beams indicate the need for a high-energy component previously absent in the photoelectron generation model. In addition, the design purpose of the shielded pickup detectors has been experimentally confirmed, as the cloud lifetime has been accurately measured using witness bunches at various delays. Sensitivity to the elastic yield parameter in the secondary yield model has been shown to be less than 0.05 and remarkably robust against variation of other model parameters. Data taken with an uncoated aluminum chamber provide a best estimate for the elastic yield of about 0.75. The cloud lifetime studies in a titanium-nitride-coated aluminum chamber exclude such a high value, yielding an optimal value of 0.05.

## REFERENCES

[1] G.F. Dugan, M.A. Palmer, and D.L. Rubin, *ILC Damping Rings R&D at CesrTA*, ICFA Beam Dynamics Newsletter No. 50, eds. J. Urakawa and W. Chou (2009)

[2] J.R. Calvey *et al.*, *Methods for Quantitative Interpretation of Retarding Field Analyzer Data*, these proceedings

[3] F. Zimmermann and G. Rumolo, *Electron Cloud Effects in Accelerators*, ICFA Beam Dynamics Newsletter No. 33, eds. K. Ohmi and M.A. Furman (2004)

[4] J.A. Crittenden *et al.*, *Studies of the Effects of Electron Cloud Formation on Beam Dynamics at CesrTA*, proceedings of PAC09, 4-8 May 2009, Vancouver, British Columbia, Canada

[5] J.A. Crittenden *et al.*, *Progress in Studies of Electron-Cloud-Induced Optics Distortions at CesrTA*, proceedings of IPAC10, 2010, Kyoto, Japan

[6] G.F. Dugan, S. Malishuk and D.C. Sagan, *SYNRAD3D Pho-*

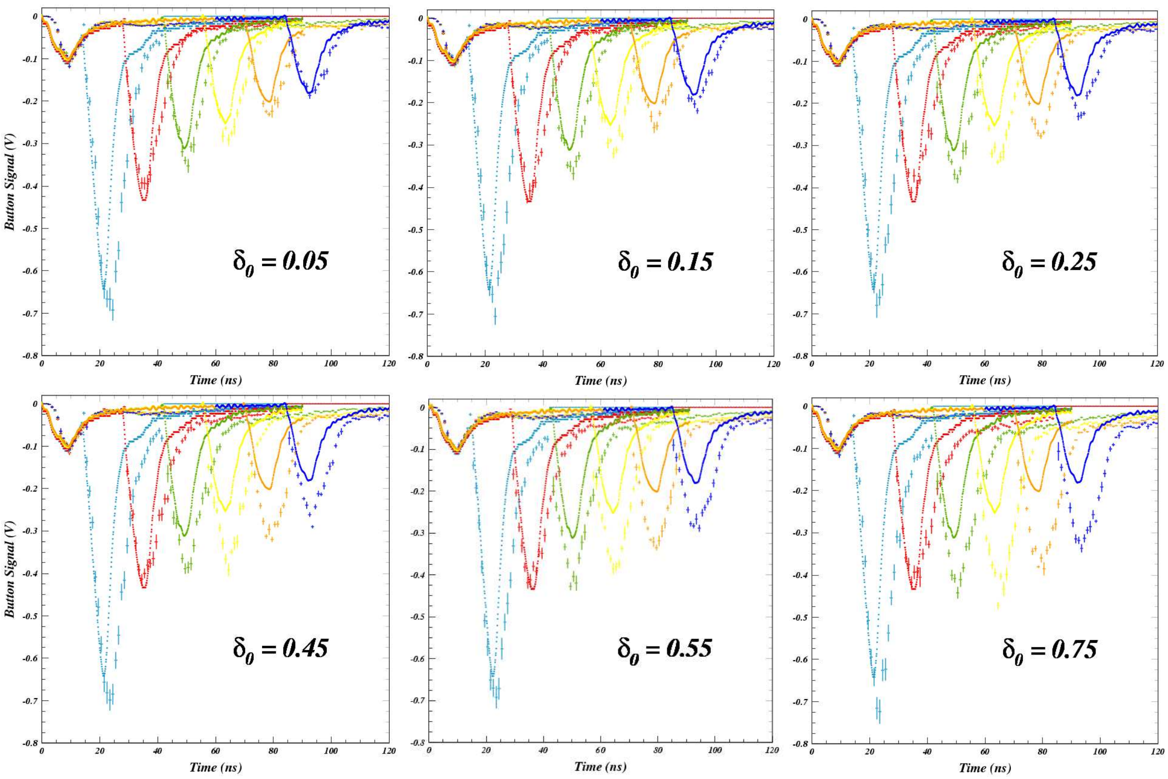


Figure 8: Witness bunch study with the titanium-nitride-coated aluminum chamber. The smooth curves are the digitized shield pickup signals. Six two-bunch scope traces are superposed in each of the six plots, whereby the delay of the witness bunch ranges from 14 to 84 ns. The magnitudes of the modeled signals at large witness bunch delay clearly show the dependence on the elastic yield parameter $\delta_0$ as it is varied from 0.05 to 0.95. The most consistent description of the measured signals is given by a value of $\delta_0 = 0.05$.


*ton Propagation and Scattering Simulation*, these proceedings

[7] G.F. Dugan, private communication

[8] U. Iriso and G. Rumolo, *Benchmarking Electron Cloud Data With Computer Simulation Codes*, proceedings of EPAC 2006, Edinburgh, Scotland

[9] M.A. Furman and M.T.F. Pivi, *Probabilistic Model for the Simulation of Secondary Electron Emission*, Phys Rev ST-AB 5, 124404 (2002)